https://doi.org/10.5194/egusphere-2023-1605
Preprint. Discussion started: 15 August 2023

Global and Indian precipitation responses to anthropogenic aerosol and carbon dioxide forcings from PDRMIP experiments

Sushant Das[1,2*], Frida Bender[1], Thorsten Mauritsen[1]

[1]Department of Meteorology, Stockholm University
Stockholm, Sweden

[2]Department of Earth and Atmospheric Sciences, National Institute of Technology Rourkela, Odisha, India

*Corresponding author: sushant.das@misu.su.se

https://doi.org/10.5194/egusphere-2023-1605
Preprint. Discussion started: 15 August 2023

Abstract

Global precipitation change in response to climate change is closely related to surface temperature, the forcing agent and the atmospheric dry energy budget, but regional precipitation change is more complex. In this study we use experiments from the Precipitation Driver and Response Model Intercomparison Project (PDRMIP) wherein carbon dioxide, sulfate aerosols and black carbon aerosols are perturbed to study the global precipitation response in contrast with the regional response over India. The response to global warming from carbon dioxide increases precipitation both globally and regionally, whereas the cooling response to sulfate aerosol leads to a reduction in precipitation in both cases. The response to black carbon aerosols, however, is a global decrease but a regional increase of precipitation over India. The mechanism is increased atmospheric heating driving a stronger monsoon circulation and stronger low level winds. This intensification of the Indian monsoon is, somewhat surprisingly, stronger for global black carbon emissions than when the emissions are limited to those from the Asian region. Overall, our study presents heterogeneity in precipitation responses at both global and regional levels and the potential underlying physical processes under a variety of climate forcings that would be useful in designing further model experiments with higher spatial resolution.

Keywords: aerosols, precipitation, PDRMIP, Indian monsoon, dynamics

1. Introduction

Human-induced changes in precipitation are evident in the present and in the past century (IPCC, 2023). It is well known that precipitation shows high spatial and temporal variability depending on different regions and seasons (Gu and Adler, 2022). The eco-system is dependent on water balance over the globe and any imbalance could have significant

https://doi.org/10.5194/egusphere-2023-1605
Preprint. Discussion started: 15 August 2023

effects. Precipitation is the source through which the earth replenishes its water content that drives the livelihood of the global population and its economy (Kotz et al., 2022). Several studies have been conducted to estimate the changes in the precipitation occurring in present day to future using observations and modelling techniques. However, quantifying precipitation changes is challenging due to several climate forcing agents e.g., greenhouse gases, aerosols, land use changes etc. acting together. Greenhouse gases (GHGs) such as carbon dioxide are considered to be one of the main drivers of the observed temperature and precipitation change because of its warming through the greenhouse effect. The GHGs have significantly warmed the climate by 1.5°C causing frequent heat waves and extreme precipitation events over different parts of the globe (IPCC, 2023). On the other hand, the anthropogenic aerosols are short-lived pollutants that can either cool or warm the atmosphere depending upon their species and hence can change the precipitation and temperature estimates. Aerosol can affect the radiation through their direct and indirect effects. Aerosols affect the radiation budget directly by absorbing and scattering incoming solar radiation (Haywood and Boucher, 2000) and indirectly by acting cloud condensation nuclei and modifying cloud microphysical properties (Albercht, 1989; Twomey, 1974).

Extensive studies have been carried out to estimate annual precipitation responses to climate forcings at a global scale. The variability in the precipitation response is mostly governed by changes in the energy budget imposed by climate forcings (O' Gorman et al., 2011). The modulation in the energy budget could be due to both natural and anthropogenic climate forcings, and the responses could be seen in weeks to years (fast) or after many years (slow). For example, annual precipitation is found to decrease initially and then tends to increase with an increase in surface temperature due to CO_2 forcings on a global scale (Andrews and Forster, 2010). The anthropogenic aerosols have continuously evolved from the preindustrial era and are known to alter the hydrological global and local cycle through

https://doi.org/10.5194/egusphere-2023-1605
Preprint. Discussion started: 15 August 2023

influencing the dynamics that controls the precipitation (Bollasina et al., 2011). Zhao and Suzuki (2021) found that aerosols can potentially shift the Intertropical convergence zone (ITCZ) that can affect the spatial variability in the global precipitation patterns. Additionally, on the global scale, the anthropogenic aerosol tends to alter the atmospheric stability through perturbation in vertical temperature profiles and surface cooling (Li et al., 2022). Zhao and Suzuki (2019) using MIROC5.2 found a global decrease in annual precipitation due to black carbon (BC) and attributed it to negative tendency of fast precipitation response scaling with instantaneous atmospheric absorption. High amount of atmospheric cooling is noticed by injecting sulfate aerosols in the Community Earth System Model (CESM) model (Krishnamohan et al., 2019). The relative cooling due to sulfate aerosols decrease the precipitation over the northern hemisphere resulting in southward migration of the ITCZ (Hwang et al., 2013)

In general, it is found that anthropogenic aerosols decrease the global precipitation due to their overall cooling effect, but the decrease is not consistent uniformly across the globe and there is significant modulation with opposite response in various regions. It is mostly due to regional dynamics that plays a crucial role in determining the precipitation response. Therefore, investigating precipitation changes on a regional scale is necessary. The regional changes could be more amplified or dampened than the global changes due to these climate drivers. From a regional point of view, monsoon systems are widely seen to be highly impacted by anthropogenic aerosols (Monerie et al., 2022, Wang et al., 2009). The heterogeneity in aerosol spatial distribution over highly polluted regions such as the South and East Asian regions could trigger changes in the distribution of monsoonal precipitation (Ganguly et al. 2012, Dong et al., 2019). The Indian Summer Monsoon (ISM) season is one of the strongest monsoons that contribute to nearly 80% of the annual precipitation during the summer months from June to September (JJAS) over India (Dash et al., 2009). The strength

https://doi.org/10.5194/egusphere-2023-1605
Preprint. Discussion started: 15 August 2023

of ISM precipitation depends both on land-sea thermal contrast and on interhemispheric temperature differences (Jin and Wang, 2017). Any perturbation over the land or sea could affect thermal and dynamical processes leading to changes in the characteristics of monsoon precipitation. Ramanathan et al., (2005) first pointed out that aerosol induced solar dimming over the northern Indian Ocean could weaken the land sea contrast and reduce the precipitation during monsoon season. Bollasina et al., (2011) attributed the weakening of meridional circulations due to anthropogenic aerosols to the decrease in precipitation during the summer season. On the contrary, aerosol induced heating over the Tibetan Plateau (Lau et al., 2006) and the tropospheric layer along the Himalayan foothills can facilitate moisture transport from the adjoining seas leading to increase in precipitation over India following Lau and Kim (2006) 'Elevated Heat Pump' hypothesis. Additionally, natural aerosols like mineral dust can increase precipitation over India both remotely as well as locally through their dynamical effects (Vinoj et al., 2014, Das et al., 2020). In terms of anthropogenic aerosol species, sulfate has been found to be more strongly related with the precipitation decrease compared to BC as shown by Guo et al., (2016). They also found that BC amplifies the radiative warming that enhances precipitation over northern India. Similar results were reported by Menon et al., (2002) where both an increase and a decrease in precipitation due to BC are noticed over different subregions of India. Very few studies examined the fast and slow responses of anthropogenic aerosols during the ISM, but Ganguly et al., (2012) using CESM found that the feedbacks associated with the sea surface temperature (SST) play a more important role than atmospheric absorption. The aerosol induced SST cooling slows down the Hadley circulation due to which lesser moisture transport occurs toward the Indian landmass thereby decreasing the ISM precipitation.

It is evident from previous studies that aerosols are critical in determining the fate of global and regional precipitation due to inhomogeneity in aerosol climate forcings. However,

https://doi.org/10.5194/egusphere-2023-1605
Preprint. Discussion started: 15 August 2023

most of these studies examined the fast responses of precipitation and the associated dynamics to aerosol forcings as the simulations varied from few years to 30 years due to computational constraints. Also, most experiment designs are performed commonly with atmospheric models where there is no interaction between atmosphere and ocean. This limits our understanding as the response of sea surface temperature (SST) to anthropogenic aerosols or slow responses is neglected. Moreover, the signals obtained by using a single model for the study may lack robustness in attributing climate responses to the anthropogenic aerosol forcings. To obtain the total responses of anthropogenic aerosols, at least a hundred years of aerosol perturbed simulations in a fully coupled or slab ocean model configuration is required. In order to address this issue, a Precipitation Driver and Response Model Intercomparison Project (PDRMIP) is designed where several model institutions partnered to carry out simulations forced with individual climate forcers. To quantify the response to various climate forcings, dedicated experiments were designed to identify the precipitation responses (Myhre et al., 2017). Some studies have already been carried out to quantify the global climate signals due to aerosol and greenhouse gases forcings using PDRMIP suite of perturbed experiments (Samset et al., 2016, Liu et al., 2018, Misios et al., 2021). Very few studies have been carried out to identify responses on a regional scale, especially in the Indian subcontinent. Only a single study using PDRMIP models, Sherman et al., (2021) found ISM precipitation to be sensitive to Indian and Chinese aerosol emissions. They also pointed out that the role of BC in modulating precipitation over India is highly uncertain. However, the changes in the precipitation in relation to changes in near surface temperature, dry energy budget and dynamics are not investigated. Additionally, the intercomparison between the global and Indian precipitation responses is needed to understand the heterogeneity in the responses due to different anthropogenic aerosol types as well as carbon dioxide forcings.

https://doi.org/10.5194/egusphere-2023-1605
Preprint. Discussion started: 15 August 2023

To fill these gaps, we extensively carried out comparative analysis to answer three primary questions. What are the characteristics of annual precipitation change on global scale and over India in response to aerosol and carbon dioxide forcing respectively? What governs precipitation on global scale and in India? What physical mechanisms could explain the ISM precipitation changes due to aerosol and carbon dioxide forcing? All these questions are addressed here by using the PDRMIP simulated model outputs through several perturbed experiments as described in the next section. In Section 3, we present and discuss the results, and Section 4 presents our main conclusion.

2. Methodology

In this paper, we procure monthly data variables from the PDRMIP project to examine the precipitation responses to aerosols as well as carbon dioxide forcings. 11 coupled models participated in the project to carry out a base simulation for each global and regional perturbed experiment (Myhre et al., 2017). Regional perturbed experiments are carried out by changing aerosol emissions or concentrations in Europe (35°–70°N, 10°W–40°E) and Asia (10°–50°N, 60°–140°E) in the models. These regional experiments include changing the BC and sulfate emissions across Europe and Asia to understand regional precipitation responses, as well as to identify their remote effects. The details of the models and their configurations used in the study are shown in Table 1. We study eight perturbed experiments performed by PDRMIP models in our study as shown in Table 2. The experiments are i) $co_2 \times 2$, ii) *bc×10*, iii) *sul×5*, iv) *bc×10asia*, v) *sul×10asia*, vi) *sul×10eur*, vii) *sulasiared* and viii) *sulred* and the responses are detected by taking the difference between the perturbed experiment and baseline simulations.

As noticed in Table 1, each model has an interactive ocean component coupled with the atmosphere and its composition. All the models do consider the aerosol direct effects. Out

https://doi.org/10.5194/egusphere-2023-1605
Preprint. Discussion started: 15 August 2023

of 11 models, 2 models viz. GISS-E2-R and MPI-ESM do not consider the aerosol indirect effects. Besides, 3 models viz. NorESM1, NCAR-CESM-CAM5 and MIROC-SPINTARS also consider BC treatments on snow (Stjern et al., 2019). It should be noted that aerosol physics and the representation of the aerosol emission/concentration could differ in the participating models causing variability in the precipitation estimates.

Though the PDRMIP project provides simulations with the fixed SSTs (sea-surface temperatures), to identify the fast responses, we focus to determine the total responses (i.e., fast + slow responses). Therefore, we consider the last 50 years of each coupled model experiment to quantify the total responses to climate forcings (Myhre et al., 2017). Some models did not carry out all experiments (Table 2) and do not have variables that are required for analysis, as mentioned in Table 3. For the ensemble analysis, we interpolated all the model data grids into 1° × 1° resolution. We intercompare the annual precipitation responses to changes in the near-surface temperature, dry energy budget, and vertical velocity at 500 hPa in all the model experiments for both global and Indian regions in all the models. The dry energy budget in the atmosphere is computed by equation given by $(SW^{\downarrow}_{TOA} - SW^{\uparrow}_{TOA} - LW^{\uparrow}_{TOA}) + (SW^{\uparrow}_{SUR} - SW^{\downarrow}_{SUR} + LW^{\uparrow}_{SUR} - LW^{\downarrow}_{SUR} + hfss)$ where

$SW^{\downarrow}_{TOA}$ (rsdt) = TOA incident shortwave radiation

$SW^{\uparrow}_{TOA}$ (rsut) = TOA outgoing shortwave radiation

$LW^{\uparrow}_{TOA}$ (rlut) = TOA outgoing longwave radiation

$SW^{\uparrow}_{SUR}$ (rsus) = surface upwelling shortwave radiation

$SW^{\downarrow}_{SUR}$ (rsds) = surface downwelling shortwave radiation

$LW^{\uparrow}_{SUR}$ (rlus) = surface upwelling longwave radiation

$LW^{\downarrow}_{SUR}$ (rlds) = surface downwelling longwave radiation

hfss = surface upward sensible heat flux

https://doi.org/10.5194/egusphere-2023-1605
Preprint. Discussion started: 15 August 2023

The spatial variability in the patterns of annual precipitation and temperature in response to anthropogenic aerosol forcings along with the changes in the ISM precipitation and the potential physical mechanisms are presented and discussed. For changes in the ISM precipitation, the changes in the near surface temperature gradient, wind patterns at 850 hPa, meridional circulations and vertical temperature are also investigated.

3. Results and Discussion

To begin with, we show the changes in the ensemble mean of annual precipitation in all experiments relative to the base experiment (in Figure 1). It is evident that annual precipitation over tropical regions (-30°N to 30°N) is highly sensitive compared to mid-latitudes and polar regions to both carbon dioxide and anthropogenic aerosol forcings. The annual precipitation patterns and intensity differ depending on the climate forcing agents. In general, there is an increase in precipitation over most of continental land regions in $co_2 \times 2$ (Figure 1a) due to an increase in the global surface temperature (Figure 2a). Some precipitation decrease is noticed over central America specifically in Mexico and parts of Brazil. In the *bc×10* experiment (Figure 1b), precipitation mostly decreases over western Europe, and north and south America and increases over India and parts of central Africa. However, the magnitude of precipitation increase is less in India compared to that in $co_2 \times 2$. Unlike $co_2 \times 2$ and *bc×10*, a substantial decrease in precipitation is observed over India, China and Southeast Asian region in *sul×5* (Figure 1c) associated with large-scale cooling induced on land mass and over ocean (Figure 2c). The relative cooling in the northern continents inhibits the northward progression of ITCZ, and therefore an increase in precipitation is seen over southern oceans in *sul×5*. A sensitivity experiment where the sulfate emissions are reduced from present day to pre-industrial state shows increases in precipitation over India, China, central Africa and parts of north and South America (Figure 1h) and surface

https://doi.org/10.5194/egusphere-2023-1605
Preprint. Discussion started: 15 August 2023

temperature (Figure 2h). Only two models from PDRMIP viz. MIROC-SPRINTARS and HadGEM3 performed these experiments and tend to show relative increases in global precipitation with increase in surface temperature (Table 3). Reducing the sulfate aerosols enhances the surface warming as noticed in the Figure 2h, which can alter the climate sensitivity leading to various feedbacks that can cause changes in the precipitation. Overall, the responses in precipitation and surface temperature are quite opposite in *sulred* to that noticed in *sul×5*. This implies that reducing the sulfate emissions through policy implementation increases the global precipitation.

Amongst all the global forcing experiments, precipitation responses in the Indian region are quite large. In the regional perturbed experiments, *bc×10asia* causes an increase in precipitation whereas *sul×10asia* causes a decrease in precipitation over the Indian region. It is to be noted that the increase in precipitation over India is less in *bc×10asia* than when forced at a global scale (*bc×10*) implying global BC aerosols contribute more to precipitation increase than the Asian emitted BC aerosols. Simultaneously, the increase in surface temperature over the Tibetan Plateau and northern continents in *bc×10* is greater than the *bc×10asia* case (Figure 2b and 2d). Previously, Kovilakam and Mahajan, (2015) using the Community Atmosphere Model (CAM4) found that BC induced mid-latitude tropospheric heating leads to shift the location of ITCZ northward leading to increase in precipitation at the northern hemisphere. Further sensitivity experiments performed by Kovilakam and Mahajan, (2016) showed that the BC induced TOA warming linearly increases with linear increase BC aerosol burden. They further concluded that the ISM precipitation also increases linearly with an increase in BC burden. The study by Meehl et al., (2008) found increases in precipitation over India due to BC induced heating over the Tibetan Plateau mostly during March to April, but they also reported slight decrease in precipitation during the monsoon months using the Community Climate System Model, version 3 (CCSM3). In our study, we

https://doi.org/10.5194/egusphere-2023-1605
Preprint. Discussion started: 15 August 2023

used multiple coupled models that suggest a major increase in precipitation during the monsoon over India, adding robustness to the attained results presented here. In the case of sulfate aerosol experiments, global sulfate aerosols (*sul×5*) causes more decrease in surface temperature over India compared to regionally perturbed *sul×10asia* (Figure 2c and 2e). In the sulfate aerosol perturbed experiments over Europe (*sul×10eur*), a negligible decrease in precipitation (Figure 1f) is noticed globally. However, the temperature decrease is maximum over Europe (-1 to -2 K) as most of the scattering sulfate aerosol are present over Europe. Apart from sulfate reduction globally, the reduction of the sulfate over Asia (*sulasiared*) also causes an increase in precipitation over India and China (Figure 1g) and a slight increase in surface temperature (Figure 1g).

To intercompare the changes in the responses between precipitation and surface temperature on a global scale and in the Indian region in individual experiments, scatter plots for all models are shown in Figure 3. It is interesting to note that on a global scale, the change in precipitation has a strong linear relationship with the change in surface temperature (Figure 3a), whereas for the Indian region a linear relation is not clear (Figure 3b). A spread in the precipitation estimates across different models can be seen in all of the global and regional aerosol perturbation experiments. At a global scale, the increase in annual mean precipitation is mostly observed in the co_2*×2* across all models (Figure 3a). In the co_2*×2* experiments, the maximum increase in precipitation of about ~5% and the temperature of ~3.8 K is observed in HadGEM3 and the minimum increase is about ~1% and ~1.5 K in precipitation and temperature, respectively, in MIROC-SPRINTARS and GISS-E2-R models. Other models are within the range of these estimates. On the other hand, a strong decrease in precipitation (~17%) and temperature (~6.4 K) is noticed in *sul×5* experiments seen in HadGEM3 model at a global scale. The *sulred* experiment shows an increase in precipitation and temperature globally, while *bc×10* shows a decrease in precipitation despite some increase in surface

https://doi.org/10.5194/egusphere-2023-1605
Preprint. Discussion started: 15 August 2023

temperature. The regional perturbed experiments i.e., *sul×10asia* and *sul×10eur* show both a decrease in precipitation and temperature with less magnitude compared to the global perturbed experiments. Over India, a synchronous direction of change with global responses is observed in *co_2×2* and all sulfate experiments (Figure 3b). The experiments with *bc×10* and *bc×10asia* tend to have an opposite response over India compared to global responses, where the increase in precipitation is associated with an increase in temperature, which implies that regional thermodynamics plays a significant role. This becomes clearer when we look at changes in precipitation in relation to changes in dry energy budget in both the global and Indian regions (Figure 4). The linear relationship shown in Figure 4a indicates that globally precipitation, apart from temperature changes, is also driven by the changes in the dry energy budget in the atmosphere. If there is a decrease in the dry energy budget in the atmosphere, there is moisture available for cloud formation leading to precipitation e.g., in the case of *co_2×2*, and *sulred*. The *co_2×2* induced warming increases the water holding capacity of the atmosphere, leading to a decrease in dry energy budget (~-1 to -5 Wm^{-2}) and an increase in precipitation (up to 5%). Likewise, removing the scattering type aerosols in *sulred*, the atmospheric absorption of water content increases, thereby increasing the precipitation. The climate forcing agents such as sulfate aerosols induce cooling of the atmosphere mostly through their scattering effects leading to a drier state (~2-15 Wm^{-2}). In addition to atmospheric cooling, there are feedbacks generated that constrain the movement of the Hadley cells limiting the moisture transport. Therefore, a higher decrease in precipitation is noticed (Figure 1c) over the tropical regions. Overall, the changes in precipitation are strongly related to changes in dry energy budget on a global scale and this relationship does not hold for the corresponding changes over the Indian region (Figure 4b). Although in some perturbed experiments, the direction of regional changes is similar but with different magnitudes to that noticed on a global scale, there is no linearity in the responses across all

https://doi.org/10.5194/egusphere-2023-1605
Preprint. Discussion started: 15 August 2023

the models. The increase in precipitation change estimated in the case of the BC experiments and decrease in precipitation change in the case of the sulfate exhibits high variability. The responses in regional perturbed *sul×10asia* show a decrease in precipitation in some models (MIROC_SPRINTARS, HadGEM3, NorESM1, NCAR-CESM1-CAM4) despite a decrease in dry energy budget, which is inconsistent.

From our analysis it is clear that globally the precipitation responses could be driven by the changes induced in temperature and dry energy budget by the forcing agents, whereas this does not hold true for regional precipitation changes over India. Therefore, we look into the relationship between the changes in precipitation and changes in the vertical pressure velocity (*Δ*vert. velocity) at 500 hPa. Vertical pressure velocity is the manifestation of both surface and atmospheric conditions in the climate model. The warmer air rises up due to the convergence of winds at the surface to lower atmospheric levels. The atmospheric heat content can also trigger updrafts, which can uplift moisture from the lower levels to the troposphere for the formation of clouds. Looking at Figure 5a, *Δ*vert. velocity is minimal and clustered around zero for global average. Ideally, the *Δ*vert. velocity should be zero while averaging globally to conserve the mass, however, certain models do have imbalances leading to some deviations. The relationship between the changes in precipitation and *Δ*vert. velocity over the Indian region on the other hand is quite robust in all the models (Figure 5b). The negative values in the *Δ*vert. velocity indicates updrafts signifying more convective activities occurring in the co_2*×2*, *bc ×10*, *bc×10asia* and *sulred*, which enhances the precipitation. The positive values in the *Δ*vert. velocity indicate descending motion, inhibiting convective processes and leading to a decrease in the precipitation in sulfate (*sul×5*, *sul×10asia*) sets of experiments. Over India, a lot of convective activity occurs during the ISM and therefore, the precipitation responses are much larger in magnitude due to anthropogenic climate forcings compared to annual time scales (Figure S1). The reduction in

https://doi.org/10.5194/egusphere-2023-1605
Preprint. Discussion started: 15 August 2023

sulfate globally enhances the mean ISM precipitation over India. The magnitude of increase in precipitation in the *co₂×2* and *bc×10* experiments and decrease in precipitation in *sul×10asia* and *sul×5* experiments is higher than that of global perturbation experiments.

The climatological annual mean ensemble cycle of precipitation over the Indian region is shown in Figure 6a. The maximum changes in precipitation are mostly during the ISM compared to winter months in all the experiments. The reduction of sulfate aerosols on a global (*sulred*) and regional scale (*sulasiared*) increases precipitation over India the most, followed by *co₂×2* and *bc×10*. One of the key features that determine the strength of ISM is the land sea thermal contrast. The temperature gradient is calculated by taking the difference between the surface temperature on the Indian land mass (70–85°E, 10–30°N) and the western Indian Ocean (50–65°E, 5°S-10°N) following Roxy et al., (2015). Consistently, there is an increase in temperature gradient in the *sulred* and *sulasiared* experiments that facilitates more moisture transport from the Arabian Sea towards India causing the increase in precipitation over India (Figure 6b). All other experiments show a positive increase in the surface temperature gradient starting from the month of April until September. Note that the variability in the gradient depends upon the type of the aerosols and region of forcings as well as number of models that carried out similar experiments. Interestingly, there is evidence of an increase in the temperature gradient in the *sul×10eur* experiment compared to the *co₂×2* and all BC experiments but the relative increase in precipitation is less. This is because not only the surface temperature affects the dynamics but also the atmospheric heating profiles determine the circulations and moisture transport pathways leading to changes in the precipitation over India. Figure 7 show the changes in the vertical cross section of air temperature and meridional circulation in all the perturbed experiments relative to their base experiments. High warming in the troposphere is noticed in *co₂×2* with stronger updrafts over the Indian region during the ISM. The high warming at the surface and tropospheric region

https://doi.org/10.5194/egusphere-2023-1605
Preprint. Discussion started: 15 August 2023

facilitates the convective processes leading to formation of clouds, which increases the precipitation. Similar patterns of warming with updrafts are noticed in *bc×10* with higher magnitude compared to *bc×10asia* experiments. This could be reason for having lesser increase in precipitation in *bc×10asia* compared to *bc×10* during the ISM (Figure S1b and S1d). On the other hand, large atmospheric cooling is seen in *sul×5* with strong downdrafts. The atmospheric cooling inhibits the formation of convective cells that leads to cloud formations over the Indian landmass. The cooling is weaker in the case of regional increase in sulfate in *sul×10asia* (Figure 7e). In both the cases there is weakening of ISM precipitation due to both surface and atmospheric cooling as well as weaker land-sea contrast. This suggests more presence of dry air over the Indian landmass, which are relatively heavier and provide unfavourable conditions to trigger local convections. There are possible signatures of remote forcings from sulfate aerosols over Europe that also can impact on the circulations over India as seen in *sul×10eur*. The cooling existed mostly over the mid tropospheric regions over the Tibetan Plateau up to the northern part of India (Figure 7f). There is slight warming noticed over central to southern latitudinal region of India, however, the mid tropospheric cooling causes downdrafts over northern part of India leading to decrease in precipitation as noticed in Figure S1f. This is quite interesting and similar precipitation decrease over India due to sulfate aerosols was reported by Liu et al., (2018). More investigation is needed to understand the teleconnection between the European sulfate aerosol emission and their effects on Indian monsoon. Reduction in sulfate aerosols switches the atmospheric cooling to warming over the Indian landmass as seen in both *sulred* and *sulasiared*. The atmospheric warming is greater in *sulred* compared to *sulasiared* causing stronger meridional circulations over the Indian landmass, which leads to more precipitation. It is to be noted that the large increase in precipitation in *sulred* could be due to movement of ITCZ northward as well as the increase in land-sea contrast. In the *sulasiared*, the northward

https://doi.org/10.5194/egusphere-2023-1605
Preprint. Discussion started: 15 August 2023

movement of ITCZ could still be hindered as there are still sulfate aerosol emissions occurring in the northern hemisphere except Asia. Broadly from the analysis, it is noticed that the atmospheric heating or cooling is more sensitive to global aerosol forcings than regional aerosol perturbed experiments due to their larger magnitude in responses (Figure 7).

During ISM, apart from the temperature profiles and meridional circulations, the dynamics associated with transporting moisture from the adjoining seas i.e., the Arabian Sea and the Bay of Bengal is also important. The winds are stronger in the Arabian Sea relative to that over the Bay of Bengal. Evaluation analysis against ERA5 shows that multi-model ensemble mean of *base* experiments (*Base_ENS*) captures the mean wind field at 850 hPa and low level specific humidity reasonably well. The low-level jet at 850 hPa is a semi-permanent feature during the ISM, which carries moisture from the adjoining seas towards the Indian landmass as shown in Figure 8a. The winds are slightly underestimated in *Base_ENS* over the Arabian Sea and Bay of Bengal partly due to coarser resolution used in the models. The averaged low-level specific humidity (1000 to 850 hPa) is also shown in Figure 8b suggesting a large amount of moisture available over both the seas surrounding the Indian landmass. However, there are some underestimations of specific humidity, which could be due to the weaker winds in the Base_ENS. The changes induced due to the climate-forcing agents could potentially affect the low-level jet leading to changes in the precipitation distribution over the Indian landmass. Figure 9 shows the changes in the responses of the low-level jets in all the experiments relative to base experiment. It is noticed that there is a strengthening of the wind (>0.6 m s^{-1}) over the northern Arabian Sea in $co_2{\times}2$ and with a higher magnitude (>1.2 m s^{-1}) in *bc×10*. This causes an increase in the moisture transport from the Arabian Sea towards the Indian region resulting increase in precipitation. Other factors include the near-surface warming induced over the continental landmass compared to that over the Arabian Sea, which creates a thermal gradient as discussed earlier. In the *bc×10* and *bc×10asia*

https://doi.org/10.5194/egusphere-2023-1605
Preprint. Discussion started: 15 August 2023

experiment, it could be seen that there is aerosol cooling effect on surface temperature over India during ISM (Figure S1b and S1d) but still we see increase in precipitation. This is because of the tropospheric thermal gradient that creates a stronger low-level jet. In the *bc×10asia*, the strengthening of winds persists, causing an increase in precipitation. As the BC emissions are increased 10 times regionally over Asia, the warming over the Tibetan Plateau (Figure 7d) creates a pathway for moisture transport towards northern India and southern China. In the *sul×5* experiment, large-scale induced cooling weakens the land-sea contrast, leading to a weakening of wind circulation (> 1.8 ms^{-1}) over the Arabian Sea (Figure 9c), resulting in a decrease in precipitation over India. The weakening of winds is also noticed in the regional experiments, which include the *sul×10asia* and *sul×10eur*. Interestingly, the weakening in wind is greater in *sul×10asia* compared to *sul×5* during ISM. Inter-comparison in the precipitation response due to sulfate aerosols indicates that a greater decrease in precipitation occurs during ISM due to the regional increase in sulfate than the global increase in sulfate (Figure S1c and S1d). In the *sulred* experiment, since the sulfates are drastically reduced to a preindustrial state, the surface and atmospheric heating over land strengthen the winds to carry more moisture from the Arabian Sea towards India contributing to increase in precipitation.

4. Summary and Conclusions

In this paper, we used the PDRMIP models to quantify the total responses of anthropogenic aerosols and carbon dioxide forcing on global and regional annual precipitation over India. In particular, we presented the precipitation response to individual forcings of anthropogenic aerosols and carbon dioxide using coupled models. The perturbed experiments included *co_2×2*, *bc×10*, *sul×5*, *bc×10asia*, *sul×10asia*, *sul×10eur*, *sulasiared* and *sulred*, and the corresponding base experiments. The total responses were derived by considering the last 50 years of individual model simulations and contrasting them with their

https://doi.org/10.5194/egusphere-2023-1605
Preprint. Discussion started: 15 August 2023

base experiments. Until now, most studies have attributed the changes using single-model perturbing experiments. Here, we showcase a multi-model ensemble analysis as well as individual models to classify the climate signals caused by these forcings. We also identify several meteorological variables driving the changes in precipitation on both a global scale and in India. In addition, we investigated the potential dynamics associated with the total changes observed in precipitation in India during the ISM season. The main conclusions of the study are as follows: -

1. The multi-model ensemble analysis suggests that the precipitation over the tropical regions is more sensitive to both anthropogenic aerosol and carbon dioxide forcings compared to other regions. However, the response in global and Indian precipitation and associated dynamics varies according to the climate forcings.

2. On the global scale, the annual precipitation responses are mostly governed by the changes in surface temperature and dry energy budget. In fact, the global mean precipitation changes display a strong positive linear relationship with changes in surface temperature and a negative linear relationship with changes in the dry energy budget across all the perturbation experiments. Among all the experiments, the maximum increase in global precipitation is found in $co_2 \times 2$ forcings with an increase in surface temperature, while the greater decrease in precipitation is found in *sul×5* with a decrease in surface temperature. Likewise, the increase in global precipitation is found in $co_2 \times 2$ forcings with a decrease in dry energy budget and a decrease in precipitation is found in *sul×5* with an increase in dry energy budget.

https://doi.org/10.5194/egusphere-2023-1605
Preprint. Discussion started: 15 August 2023

3. The annual precipitation responses over India do not hold strong relationship with the changes in the surface temperature and dry energy budget. The changes in precipitation over India are mostly driven by the changes in vertical velocity at 500 hPa implying that regional dynamics are more important for the regional precipitation responses.

4. Contrasting effects of BC aerosols are observed when comparing precipitation responses at a global scale and over India. Globally, most of the models show decrease in annual precipitation and increase in annual and summer monsoon precipitation over India.

5. The maximum change in precipitation is found during the summer monsoon season over India. High atmospheric and surface heating induced in *co_2×2* and BC (*bc×10* and *bc×10asia*) experiments facilitate more updrafts over the Indian landmass leading to increase in precipitation during the ISM. The BC induced heating in the troposphere creates a thermal gradient that strengthens the low-level jet at 850 hPa and meridional circulation. Consequently, high atmospheric and surface cooling in *sul×5* and *sul×10asia* leads to weakening of low-level winds and downdrafts induced by cooling inhibit convective activity over India leading to decrease in precipitation during ISM.

6. Reduction of sulfate aerosols globally and over Asia increases the atmospheric warming tendency causing an increase in precipitation over India. Interestingly,

https://doi.org/10.5194/egusphere-2023-1605
Preprint. Discussion started: 15 August 2023

larger increase in precipitation is observed over India during the ISM while reducing the sulfate aerosols globally rather than only over Asia.

Acknowledgements

We thank the PDRMIP project for providing data for carrying out analysis. All the PDRMIP simulation data used in the paper are publicly available online link from the WDCC server https://www.wdc-climate.de/ui/entry?acronym=PDRMIP_2012-2021. Special thanks to Norwegian Research Infrastructure Services (NRIS) for providing us with an account to access all the data from the PDRMIP model used in the study. For analysis and plotting, we acknowledge the usage of climate data operator (CDO), python packages and GrADS. This work was funded by the European Union's Horizon 2020 research and innovation program projects NextGEMS and CONSTRAIN (Grant agreements No.101003470 and No.820829) and the European Research Council (ERC) (Grant agreement No.770765). We acknowledge support from the Swedish e-Science Research Centre (SeRC). The partly data storage was enabled by resources provided by the National Academic Infrastructure for Supercomputing in Sweden (NAISS) and the Swedish National Infrastructure for Computing (SNIC) at MISU, Stockholm University partially funded by the Swedish Research Council through grant agreements no. 2022-06725 and no. 2018-05973.

Code/Data availability

All the PDRMIP simulation data used in the paper are publicly available online link from the WDCC server https://www.wdc-climate.de/ui/entry?acronym=PDRMIP_2012-2021. For analysis and plotting, data operator (CDO), python packages and GrADS have been used.

The codes for plotting the figures are available from the corresponding author upon reasonable request.

Author contributions

SD along with FB and TM conceptualized the study. SD carried out all the analysis taking feedbacks from FB and TM. SD wrote first version of the paper and all authors contributed in preparing the final version of the draft. The funds for carrying out this study is acquired by FB and TM.

Competing interests

The corresponding author has declared that none of the authors has any competing interests.

References

Albrecht, B. A.: Aerosols, Cloud Microphysics, and Fractional Cloudiness, Science, 245, 1227–1230, https://doi.org/10.1126/science.245.4923.1227, 1989.

Andrews, T. and Forster, P. M.: The transient response of global-mean precipitation to increasing carbon dioxide levels, Environ. Res. Lett., 5, 025212, https://doi.org/10.1088/1748-9326/5/2/025212, 2010.

Bentsen, M., Bethke, I., Debernard, J. B., Iversen, T., Kirkevåg, A., Seland, Ø., Drange, H., Roelandt, C., Seierstad, I. A., Hoose, C., and Kristjánsson, J. E.: The Norwegian Earth System Model, NorESM1-M – Part 1: Description and basic evaluation of the physical climate, Geosci. Model Dev., 6, 687–720, https://doi.org/10.5194/gmd-6-687-2013, 2013.

https://doi.org/10.5194/egusphere-2023-1605
Preprint. Discussion started: 15 August 2023

Bollasina, M.A., Ming, Y., Ramaswamy, V.: Anthropogenic aerosols and the weakening of the south Asian summer monsoon. Science 334:502–506, 2011

Das, S., Giorgi, F., and Giuliani, G.: Investigating the relative responses of regional monsoon dynamics to snow darkening and direct radiative effects of dust and carbonaceous aerosols over the Indian subcontinent, Clim Dyn, 55, 1011–1030, https://doi.org/10.1007/s00382-020-05307-1, 2020.

Dash, S. K., Kulkarni, M. A., Mohanty, U. C., and Prasad, K.: Changes in the characteristics of rain events in India, J. Geophys. Res., 114, D10109, https://doi.org/10.1029/2008JD010572, 2009.

D'Errico, M., Cagnazzo, C., Fogli, P. G., Lau, W. K. M., Hardenberg, J., Fierli, F., and Cherchi, A.: Indian monsoon and the elevated-heat-pump mechanism in a coupled aerosol-climate model, J. Geophys. Res. Atmos., 120, 8712–8723, https://doi.org/10.1002/2015JD023346, 2015.

Dong, B., Wilcox, L. J., Highwood, E. J., and Sutton, R. T.: Impacts of recent decadal changes in Asian aerosols on the East Asian summer monsoon: roles of aerosol–radiation and aerosol–cloud interactions, Clim Dyn, 53, 3235–3256, https://doi.org/10.1007/s00382-019-04698-0, 2019.

Dufresne, J.-L., Foujols, M.-A., Denvil, S., Caubel, A., Marti, O., Aumont, O., Balkanski, Y., Bekki, S., Bellenger, H., Benshila, R., Bony, S., Bopp, L., Braconnot, P., Brockmann, P., Cadule, P., Cheruy, F., Codron, F., Cozic, A., Cugnet, D., de Noblet, N., Duvel, J.-P., Ethé, C., Fairhead, L., Fichefet, T., Flavoni, S., Friedlingstein, P., Grandpeix, J.-Y., Guez, L., Guilyardi, E., Hauglustaine, D., Hourdin, F., Idelkadi, A., Ghattas, J., Joussaume, S., Kageyama, M., Krinner, G., Labetoulle, S., Lahellec, A., Lefebvre, M.-P., Lefevre, F., Levy, C., Li, Z. X., Lloyd, J., Lott, F., Madec, G., Mancip, M., Marchand, M., Masson, S., Meurdesoif, Y., Mignot, J., Musat, I., Parouty, S., Polcher, J., Rio, C., Schulz, M., Swingedouw, D., Szopa, S., Talandier, C., Terray, P., Viovy, N., and Vuichard, N.: Climate change projections using the IPSL-CM5 Earth System Model: from CMIP3 to CMIP5, Clim Dyn, 40, 2123–2165, https://doi.org/10.1007/s00382-012-1636-1, 2013.

Ganguly, D., Rasch, P. J., Wang, H., and Yoon, J.-H.: Climate response of the South Asian monsoon system to anthropogenic aerosols: CLIMATE EFFECTS OF ANTHROPOGENIC AEROSOL, J. Geophys. Res., 117, n/a-n/a, https://doi.org/10.1029/2012JD017508, 2012.

Gent, P. R., Danabasoglu, G., Donner, L. J., Holland, M. M., Hunke, E. C., Jayne, S. R., Lawrence, D. M., Neale, R. B., Rasch, P. J., Vertenstein, M., Worley, P. H., Yang, Z.-L., and Zhang, M.: The Community Climate System Model Version 4, J. Climate, 24, 4973–4991, https://doi.org/10.1175/2011JCLI4083.1, 2011.

Gu, G. and Adler, R. F.: Observed variability and trends in global precipitation during 1979–2020, Clim Dyn, https://doi.org/10.1007/s00382-022-06567-9, 2022.

Guo, L., Turner, A. G., and Highwood, E. J.: Local and Remote Impacts of Aerosol Species on Indian Summer Monsoon Rainfall in a GCM, Journal of Climate, 29, 6937–6955, https://doi.org/10.1175/JCLI-D-15-0728.1, 2016.

https://doi.org/10.5194/egusphere-2023-1605
Preprint. Discussion started: 15 August 2023

Haywood, J. and Boucher, O.: Estimates of the direct and indirect radiative forcing due to tropospheric aerosols: A review, Rev. Geophys., 38, 513–543, https://doi.org/10.1029/1999RG000078, 2000.

Held, I. M. and Soden, B. J.: Robust Responses of the Hydrological Cycle to Global Warming, Journal of Climate, 19, 5686–5699, https://doi.org/10.1175/JCLI3990.1, 2006.

Hwang, Y., Frierson, D. M. W., and Kang, S. M.: Anthropogenic sulfate aerosol and the southward shift of tropical precipitation in the late 20th century, Geophys. Res. Lett., 40, 2845–2850, https://doi.org/10.1002/grl.50502, 2013.

IPCC : Summary for Policymakers. In: Climate Change 2023: Synthesis Report. A Report of the Intergovernmental Panel on Climate Change. Contribution of Working Groups I, II and III to the Sixth Assessment Report of the Intergovernmental Panel on Climate Change [Core Writing Team, H. Lee and J. Romero (eds.)]. IPCC, Geneva, Switzerland, 36 pages. (in press), 2023.

Jin, Q. and Wang, C.: A revival of Indian summer monsoon rainfall since 2002, Nature Clim Change, 7, 587–594, https://doi.org/10.1038/nclimate3348, 2017.

Kotz, M., Levermann, A., and Wenz, L.: The effect of rainfall changes on economic production, Nature, 601, 223–227, https://doi.org/10.1038/s41586-021-04283-8, 2022.

https://doi.org/10.5194/egusphere-2023-1605
Preprint. Discussion started: 15 August 2023

Kovilakam, M. and Mahajan, S.: Black carbon aerosol-induced Northern Hemisphere tropical expansion: BC AEROSOL-INDUCED TROPICAL EXPANSION, Geophys. Res. Lett., 42, 4964–4972, https://doi.org/10.1002/2015GL064559, 2015.

Kovilakam, M. and Mahajan, S.: Confronting the "Indian summer monsoon response to black carbon aerosol" with the uncertainty in its radiative forcing and beyond: BC UNCERTAINTY AND THE INDIAN MONSOON, J. Geophys. Res. Atmos., 121, 7833–7852, https://doi.org/10.1002/2016JD024866, 2016.

Krishnamohan, K.-P. S.-P., Bala, G., Cao, L., Duan, L., and Caldeira, K.: Climate system response to stratospheric sulfate aerosols: sensitivity to altitude of aerosol layer, Earth Syst. Dynam., 10, 885–900, https://doi.org/10.5194/esd-10-885-2019, 2019.

Krishna-Pillai Sukumara-Pillai, K., Bala, G., Cao, L., Duan, L., and Caldeira, K.: Climate System Response to Stratospheric Sulfate Aerosols:Sensitivity to Altitude of Aerosol Layer, Dynamics of the Earth system: concepts, https://doi.org/10.5194/esd-2019-21, 2019.

Lau, K. M., Kim, M. K., and Kim, K. M.: Asian summer monsoon anomalies induced by aerosol direct forcing: the role of the Tibetan Plateau, Clim Dyn, 26, 855–864, https://doi.org/10.1007/s00382-006-0114-z, 2006.

Lau, K.-M. and Kim, K.-M.: Observational relationships between aerosol and Asian monsoon rainfall, and circulation, Geophys. Res. Lett., 33, L21810, https://doi.org/10.1029/2006GL027546, 2006.

https://doi.org/10.5194/egusphere-2023-1605
Preprint. Discussion started: 15 August 2023

Li, J., Carlson, B. E., Yung, Y. L., Lv, D., Hansen, J., Penner, J. E., Liao, H., Ramaswamy, V., Kahn, R. A., Zhang, P., Dubovik, O., Ding, A., Lacis, A. A., Zhang, L., and Dong, Y.: Scattering and absorbing aerosols in the climate system, Nat Rev Earth Environ, 3, 363–379, https://doi.org/10.1038/s43017-022-00296-7, 2022.

Liu, L., Shawki, D., Voulgarakis, A., Kasoar, M., Samset, B. H., Myhre, G., Forster, P. M., Hodnebrog, Ø., Sillmann, J., Aalbergsjø, S. G., Boucher, O., Faluvegi, G., Iversen, T., Kirkevåg, A., Lamarque, J.-F., Olivié, D., Richardson, T., Shindell, D., and Takemura, T.: A PDRMIP Multimodel Study on the Impacts of Regional Aerosol Forcings on Global and Regional Precipitation, Journal of Climate, 31, 4429–4447, https://doi.org/10.1175/JCLI-D-17-0439.1, 2018.

Mahajan, S., Evans, K. J., Hack, J. J., and Truesdale, J. E.: Linearity of Climate Response to Increases in Black Carbon Aerosols, Journal of Climate, 26, 8223–8237, https://doi.org/10.1175/JCLI-D-12-00715.1, 2013.

Martin G.M, Bellouin, N., Collins, W. J., Culverwell, I. D., Halloran, P. R., Hardiman, S. C., Hinton, T. J., Jones, C. D., McDonald, R. E., McLaren, A. J., O'Connor, F. M., Roberts, M. J., Rodriguez, J. M., Woodward, S., Best, M. J., Brooks, M. E., Brown, A. R., Butchart, N., Dearden, C., Derbyshire, S. H., Dharssi, I., Doutriaux-Boucher, M., Edwards, J. M., Falloon, P. D., Gedney, N., Gray, L. J., Hewitt, H. T., Hobson, M., Huddleston, M. R., Hughes, J., Ineson, S., Ingram, W. J., James, P. M., Johns, T. C., Johnson, C. E., Jones, A., Jones, C. P., Joshi, M. M., Keen, A. B., Liddicoat, S., Lock, A. P., Maidens, A. V., Manners, J. C., Milton, S. F., Rae, J. G. L., Ridley, J. K., Sellar, A., Senior, C. A., Totterdell, I. J., Verhoef, A., Vidale, P. L., and Wiltshire, A.: The HadGEM2 family of Met Office Unified Model climate

https://doi.org/10.5194/egusphere-2023-1605
Preprint. Discussion started: 15 August 2023

configurations, Geosci. Model Dev., 4, 723–757, https://doi.org/10.5194/gmd-4-723-2011, 2011.

Meehl, G. A., Arblaster, J. M., and Collins, W. D.: Effects of Black Carbon Aerosols on the Indian Monsoon, Journal of Climate, 21, 2869–2882, https://doi.org/10.1175/2007JCLI1777.1, 2008.

Menon, S., Hansen, J., Nazarenko, L., and Luo, Y.: Climate Effects of Black Carbon Aerosols in China and India, Science, 297, 2250–2253, https://doi.org/10.1126/science.1075159, 2002.

Misios, S., Kasoar, M., Kasoar, E., Gray, L., Haigh, J., Stathopoulos, S., Kourtidis, K., Myhre, G., Olivié, D., Shindell, D., and Tang, T.: Similar patterns of tropical precipitation and circulation changes under solar and greenhouse gas forcing, Environ. Res. Lett., 16, 104045, https://doi.org/10.1088/1748-9326/ac28b1, 2021.

Monerie, P.-A., Wilcox, L. J., and Turner, A. G.: Effects of Anthropogenic Aerosol and Greenhouse Gas Emissions on Northern Hemisphere Monsoon Precipitation: Mechanisms and Uncertainty, Journal of Climate, 35, 2305–2326, https://doi.org/10.1175/JCLI-D-21-0412.1, 2022.

Myhre, G., Samset, B., Forster, P. M., Hodnebrog, Ø., Sandstad, M., Mohr, C. W., Sillmann, J., Stjern, C. W., Andrews, T., Boucher, O., Faluvegi, G., Iversen, T., Lamarque, J.-F., Kasoar, M., Kirkevåg, A., Kramer, R., Liu, L., Mülmenstädt, J., Olivié, D., Quaas, J., Richardson, T. B., Shawki, D., Shindell, D., Smith, C., Stier, P., Tang, T., Takemura, T.,

https://doi.org/10.5194/egusphere-2023-1605
Preprint. Discussion started: 15 August 2023

Voulgarakis, A., and Watson-Parris, D.: Scientific data from precipitation driver response model intercomparison project, Sci Data, 9, 123, https://doi.org/10.1038/s41597-022-01194-9, 2022.

O'Gorman, P. A., Allan, R. P., Byrne, M. P., and Previdi, M.: Energetic Constraints on Precipitation Under Climate Change, Surv Geophys, 33, 585–608, https://doi.org/10.1007/s10712-011-9159-6, 2012.

Otto-Bliesner, B. L., Brady, E. C., Fasullo, J., Jahn, A., Landrum, L., Stevenson, S., Rosenbloom, N., Mai, A., and Strand, G.: Climate Variability and Change since 850 CE: An Ensemble Approach with the Community Earth System Model, Bulletin of the American Meteorological Society, 97, 735–754, https://doi.org/10.1175/BAMS-D-14-00233.1, 2016.

Ramanathan, V., Chung, C., Kim, D., Bettge, T., Buja, L., Kiehl, J. T., Washington, W. M., Fu, Q., Sikka, D. R., and Wild, M.: Atmospheric brown clouds: Impacts on South Asian climate and hydrological cycle, Proc. Natl. Acad. Sci. U.S.A., 102, 5326–5333, https://doi.org/10.1073/pnas.0500656102, 2005.

Roeckner, E., Bäuml, G., Bonaventura, L., Brokopf, R., Esch, M., Giorgetta, M., Hagemann, S., Kirchner, I., Kornblueh, L., Manzini, E., Rhodin, A., Schlese, U., Schulzweida, U., and Tompkins, A.: The atmospheric general circulation model ECHAM5 - Part I: Model description, Technical report, 2003

https://doi.org/10.5194/egusphere-2023-1605
Preprint. Discussion started: 15 August 2023

Roxy, M. K., Ghosh, S., Pathak, A., Athulya, R., Mujumdar, M., Murtugudde, R., Terray, P., and Rajeevan, M.: A threefold rise in widespread extreme rain events over central India, Nat Commun, 8, 708, https://doi.org/10.1038/s41467-017-00744-9, 2017.

Samset, B. H., Myhre, G., Forster, P. M., Hodnebrog, Ø., Andrews, T., Faluvegi, G., Fläschner, D., Kasoar, M., Kharin, V., Kirkevåg, A., Lamarque, J. F., Olivié, D., Richardson, T., Shindell, D., Shine, K. P., Takemura, T., and Voulgarakis, A.: Fast and slow precipitation responses to individual climate forcers: A PDRMIP multimodel study, Geophys. Res. Lett., 43, 2782–2791, https://doi.org/10.1002/2016GL068064, 2016.

Samset, B. H., Lund, M. T., Bollasina, M., Myhre, G., and Wilcox, L.: Emerging Asian aerosol patterns, Nat. Geosci., 12, 582–584, https://doi.org/10.1038/s41561-019-0424-5, 2019.

Schmidt, G. A., Kelley, M., Nazarenko, L., Ruedy, R., Russell, G. L., Aleinov, I., Bauer, M., Bauer, S. E., Bhat, M. K., Bleck, R., Canuto, V., Chen, Y.-H., Cheng, Y., Clune, T. L., Del Genio, A., de Fainchtein, R., Faluvegi, G., Hansen, J. E., Healy, R. J., Kiang, N. Y., Koch, D., Lacis, A. A., LeGrande, A. N., Lerner, J., Lo, K. K., Matthews, E. E., Menon, S., Miller, R. L., Oinas, V., Oloso, A. O., Perlwitz, J. P., Puma, M. J., Putman, W. M., Rind, D., Romanou, A., Sato, M., Shindell, D. T., Sun, S., Syed, R. A., Tausnev, N., Tsigaridis, K., Unger, N., Voulgarakis, A., Yao, M.-S., and Zhang, J.: Configuration and assessment of the GISS ModelE2 contributions to the CMIP5 archive: GISS MODEL-E2 CMIP5 SIMULATIONS, J. Adv. Model. Earth Syst., 6, 141–184, https://doi.org/10.1002/2013MS000265, 2014.

Sherman, P., Gao, M., Song, S., Archibald, A. T., Abraham, N. L., Lamarque, J.-F., Shindell, D., Faluvegi, G., and McElroy, M. B.: Sensitivity of modeled Indian monsoon to Chinese and Indian aerosol emissions, Atmos. Chem. Phys., 21, 3593–3605, https://doi.org/10.5194/acp-21-3593-2021, 2021.

Stevens, B., Giorgetta, M., Esch, M., Mauritsen, T., Crueger, T., Rast, S., Salzmann, M., Schmidt, H., Bader, J., Block, K., Brokopf, R., Fast, I., Kinne, S., Kornblueh, L., Lohmann, U., Pincus, R., Reichler, T., and Roeckner, E.: Atmospheric component of the MPI□M Earth System Model: ECHAM6, J. Adv. Model. Earth Syst., 5, 146–172, https://doi.org/10.1002/jame.20015, 2013.

Stjern, C. W., Lund, M. T., Samset, B. H., Myhre, G., Forster, P. M., Andrews, T., Boucher, O., Faluvegi, G., Fläschner, D., Iversen, T., Kasoar, M., Kharin, V., Kirkevåg, A., Lamarque, J., Olivié, D., Richardson, T., Sand, M., Shawki, D., Shindell, D., Smith, C. J., Takemura, T., and Voulgarakis, A.: Arctic Amplification Response to Individual Climate Drivers, J. Geophys. Res. Atmos., 124, 6698–6717, https://doi.org/10.1029/2018JD029726, 2019.

Takahashi, H. G., Watanabe, S., Nakata, M., and Takemura, T.: Response of the atmospheric hydrological cycle over the tropical Asian monsoon regions to anthropogenic aerosols and its seasonality, Prog Earth Planet Sci, 5, 44, https://doi.org/10.1186/s40645-018-0197-2, 2018.

Takemura, T.: Return to different climate states by reducing sulphate aerosols under future CO2 concentrations, Sci Rep, 10, 21748, https://doi.org/10.1038/s41598-020-78805-1, 2020.

Twomey, S.,: Pollution and the planetary albedo.Atmospheric Environment,8, 1251–1256, 1974

Vinoj, V., Rasch, P. J., Wang, H., Yoon, J.-H., Ma, P.-L., Landu, K., and Singh, B.: Short-term modulation of Indian summer monsoon rainfall by West Asian dust, Nature Geosci, 7, 308–313, https://doi.org/10.1038/ngeo2107, 2014.

Walters, D. N., Williams, K. D., Boutle, I. A., Bushell, A. C., Edwards, J. M., Field, P. R., Lock, A. P., Morcrette, C. J., Stratton, R. A., Wilkinson, J. M., Willett, M. R., Bellouin, N., Bodas-Salcedo, A., Brooks, M. E., Copsey, D., Earnshaw, P. D., Hardiman, S. C., Harris, C. M., Levine, R. C., MacLachlan, C., Manners, J. C., Martin, G. M., Milton, S. F., Palmer, M. D., Roberts, M. J., Rodríguez, J. M., Tennant, W. J., and Vidale, P. L.: The Met Office Unified Model Global Atmosphere 4.0 and JULES Global Land 4.0 configurations, Geosci. Model Dev., 7, 361–386, https://doi.org/10.5194/gmd-7-361-2014, 2014.

Watanabe, M., Suzuki, T., O'ishi, R., Komuro, Y., Watanabe, S., Emori, S., Takemura, T., Chikira, M., Ogura, T., Sekiguchi, M., Takata, K., Yamazaki, D., Yokohata, T., Nozawa, T., Hasumi, H., Tatebe, H., and Kimoto, M.: Improved Climate Simulation by MIROC5: Mean States, Variability, and Climate Sensitivity, Journal of Climate, 23, 6312–6335, https://doi.org/10.1175/2010JCLI3679.1, 2010.

Wilcox, L. J., Liu, Z., Samset, B. H., Hawkins, E., Lund, M. T., Nordling, K., Undorf, S., Bollasina, M., Ekman, A. M. L., Krishnan, S., Merikanto, J., and Turner, A. G.: Accelerated increases in global and Asian summer monsoon precipitation from future aerosol reductions, Atmos. Chem. Phys., 20, 11955–11977, https://doi.org/10.5194/acp-20-11955-2020, 2020.

https://doi.org/10.5194/egusphere-2023-1605
Preprint. Discussion started: 15 August 2023

Xie, X., Myhre, G., Shindell, D., Faluvegi, G., Takemura, T., Voulgarakis, A., Shi, Z., Li, X., Xie, X., Liu, H., Liu, X., and Liu, Y.: Anthropogenic sulfate aerosol pollution in South and East Asia induces increased summer precipitation over arid Central Asia, Commun Earth Environ, 3, 328, https://doi.org/10.1038/s43247-022-00660-x, 2022.

Zhao, S. and Suzuki, K.: Exploring the Impacts of Aerosols on ITCZ Position Through Altering Different Autoconversion Schemes and Cumulus Parameterizations, Geophys Res Atmos, 126, https://doi.org/10.1029/2021JD034803, 2021.

https://doi.org/10.5194/egusphere-2023-1605
Preprint. Discussion started: 15 August 2023

Tables

Model, (version) reference	**Horizontal resolution, (vertical levels)**	**Ocean coupling**	**Aerosol setup**
MIROC-SPRINTARS, (5.9.0)-Watanabe et al. (2010)	1.4° × 1.4°, (40)	Coupled	HTAP2 emissions
NorESM1, (NorESM1-M, Intermediate resolution) Bentsen et al. (2013)	2.5° × 1.9°, (26)	Coupled	Fixed concentrations
NCAR-CESM1-CAM5, (1.1.2) Otto-Bliesner et al. (2016)	2.5° × 1.9° (30)	Coupled	Emissions
HadGEM2, (6.6.3) Martin et al. (2011)	1.875°×1.25° (38)	Coupled	Emissions
HadGEM3, (GA 4.0) Walters et al. (2014)	1.875°×1.25° (85)	Coupled	Fixed concentrations
GISS-E2-R, (E2-R) Schmidt et al. (2014)	2° × 2.5° (40)	Coupled	Fixed concentrations
NCAR-CESM1-CAM4, (1.0.3) Gent et al. (2011)	2.5° × 1.9° (26)	Slab ocean	Fixed concentrations
CanESM2, (2010) Arora et al. (2011)	2.8° × 2.8° (35)	Coupled	Emissions
ECHAM-HAM (6.3) Roeckner et al. (2003)	1.875°×1.875° (17)	Slab ocean	Emissions
MPI-ESM, (1.1.00p2) Stevens et al. (2013)	T63 (47)	Coupled	Climatology year 2000
IPSL-CM5A, (CMIP5) Dufresne et al. (2013)	3.75°×1.875° (39)	Coupled	Fixed concentration

Table 1: Description of the 11 models used from the Precipitation Driver Model Intercomparison Project. HTAP2 is the Hemispheric Transport Air Pollution, phase 2. The usage of emissions or concentrations of carbon dioxide and anthropogenic aerosols as input depends upon the inbuilt model type configurations for carrying out simulations.

https://doi.org/10.5194/egusphere-2023-1605
Preprint. Discussion started: 15 August 2023

Experiment	**Details**
base	All anthropogenic and natural climate forcings agents at present day or pre-industrial abundances.
co_2×2	Doubling of CO_2 concentration relative to base experiment.
bc×10	Increase in the anthropogenic black carbon concentrations or emissions by 10 times relative to base experiment
sul×5	Increase in the anthropogenic sulfate emissions by 10 times relative to base experiment.
bc×10asia	Increase in the black carbon present day concentrations 10 times over Asia only.
sul×10asia	Increase in the sulfate present day concentrations 10 times over Asia only.
sul×10eur	Increase in the sulfate present day concentrations 10 times over Europe only.
sulasiared	Sulfate concentration from present-day to pre-industrial concentration over Asia only.
sulred	Sulfate concentration from present-day to pre-industrial concentration globally.

Table 2: List of PDRMIP model experiments performed with coupled model configurations used in the study.

https://doi.org/10.5194/egusphere-2023-1605
Preprint. Discussion started: 15 August 2023

Model	Experiments	Variables used
MIROC-SPRINTARS	base, co_2×2, bc×10, sul×5, bc×10asia, sul×10asia, sul×10eur, sulasiared, sulred	pr, tas, ta, wap, ua, va, rsdt, rsut, rlut, rsus, rsds, rlus, rlds, hfss
NorESM1	base, co_2×2, bc×10, sul×5, bc×10asia, sul×10asia, sul×10eur	pr, tas, ta, wap, ua, va, rsdt, rsut, rlut, rsus, rsds, rlus, rlds, hfss
NCAR-CESM1-CAM5	base, co_2×2, bc×10, sul×5, bc×10asia, sul×10asia, sul×10eur	pr, tas, ta, wap, ua, va, rsdt, rsut, rlut, rsus, rsds, rlus, rlds, hfss
HadGEM2	base, co_2×2, bc×10, sul×5	pr, tas, ta, wap, ua, va, rsdt, rsut, rlut, rsus, rsds, rlus, rlds, hfss
HadGEM3	base, co_2×2, bc×10, sul×5, bc×10asia, sul×10asia, sul×10eur, sulred	pr, tas, ta, wap, ua, va, rsdt, rsut, rlut, rsus, rsds, rlus, rlds, hfss
GISS-E2-R	base, co_2×2, bc×10, sul×5, bc×10asia, sul×10asia, sul×10eur	pr, tas, ta, wap, ua, va, rsdt, rsut, rlut, rsus, rsds, rlus, rlds, hfss
NCAR-CESM1-CAM4	base, co_2×2, bc×10, sul×5, sul×10asia, sul×10eur	pr, tas, ta, wap, ua, va, rsdt, rsut, rlut, rsus, rsds, rlus, rlds, hfss
CanESM2	base, co_2×2, bc×10, sul×5	pr, tas, ta, wap, ua, va, rsdt, rsut, rlut, rsus, rsds, rlus, rlds, hfss
ECHAM-HAM	base, co_2×2, bc×10	pr, tas, ta, wap, ua, va, rsdt, rsut, rlut, rsus, rsds, rlus, rlds, hfss
MPI-ESM	base, co_2×2	pr, tas, ta, wap, ua, va, rsdt, rsut, rlut, rsus, rsds, rlus, rlds, hfss
IPSL-CM5A	base, co_2×2, bc×10, sul×5, bc×10asia, sul×10asia, sul×10eur	pr, tas, ua, va

Table 3: List of experiments performed by the PDRMIP models and variable simulated.

https://doi.org/10.5194/egusphere-2023-1605
Preprint. Discussion started: 15 August 2023

Variable used from PDRMIP models (short name)	**Long name**
pr	Total precipitation
tas	Near surface temperature
ta	Air temperature
wap	Vertical component of velocity (omega)
ua	Zonal component of velocity
va	Meridional component of velocity
rsdt	TOA incident shortwave radiation
rsut	TOA outgoing shortwave radiation
rlut	TOA outgoing longwave radiation
rsus	Surface upwelling shortwave radiation
rsds	Surface downwelling shortwave radiation
rlus	Surface upwelling longwave radiation
rlds	Surface downwelling longwave radiation
hfss	Surface upward sensible heat flux

Table 4: list of variables and their long name utilised in our study.

https://doi.org/10.5194/egusphere-2023-1605
Preprint. Discussion started: 15 August 2023

Figures

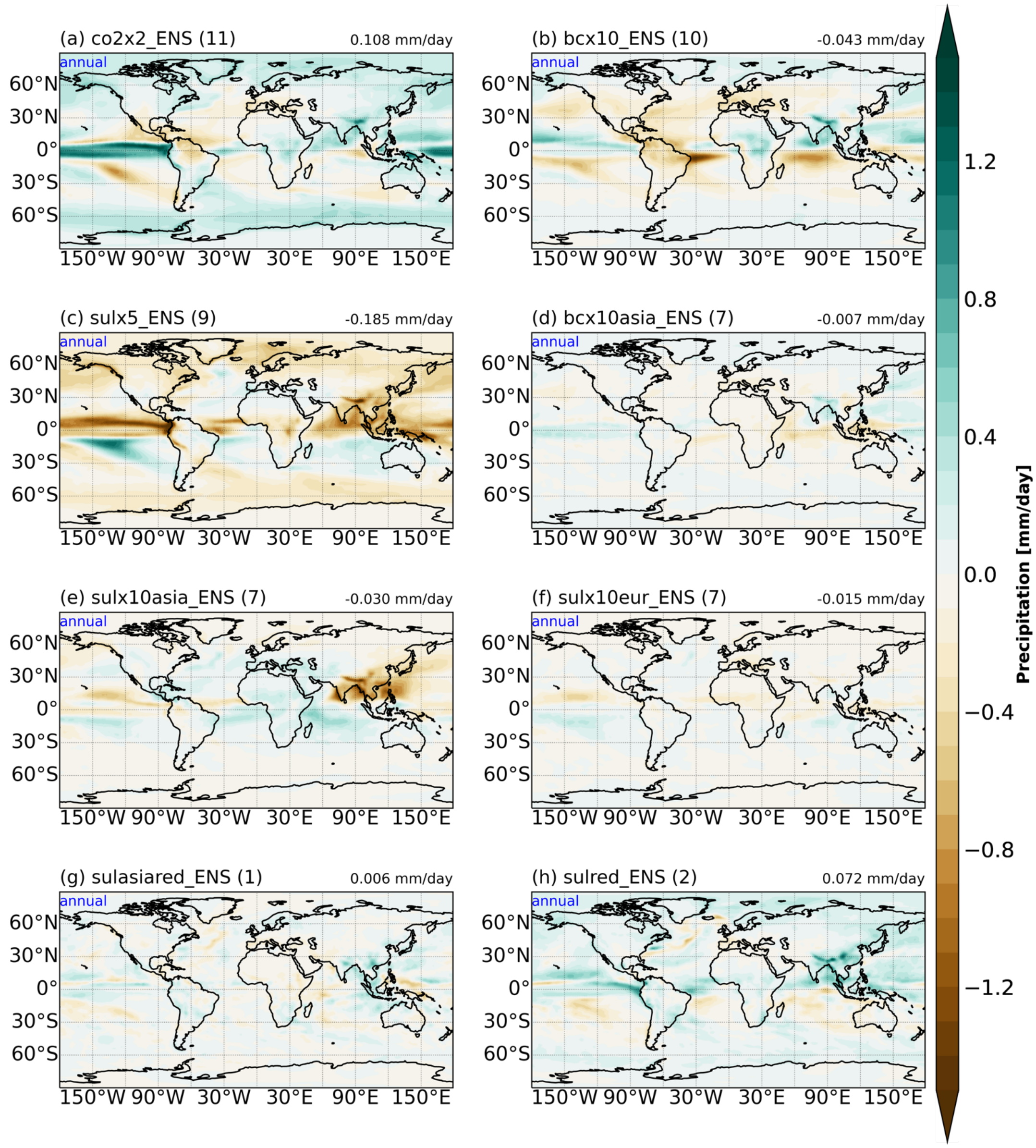

Figure 1: Spatial distribution of ensemble mean of annual total precipitation responses (mm/day) in (a) *co₂×2*, (b) *bc×10*, (c) *sul×5*, (d) *bc×10asia*, (e) *sul×10asia*, (f) *sul×10eur*, (g) *sulasiared* and (h) *sulred* with respect to their base experiments. The values in the brackets represent number of models carried out the experiment. The ensemble mean of change in annual precipitation for each perturbed experiment is given on the top right corner.

https://doi.org/10.5194/egusphere-2023-1605
Preprint. Discussion started: 15 August 2023

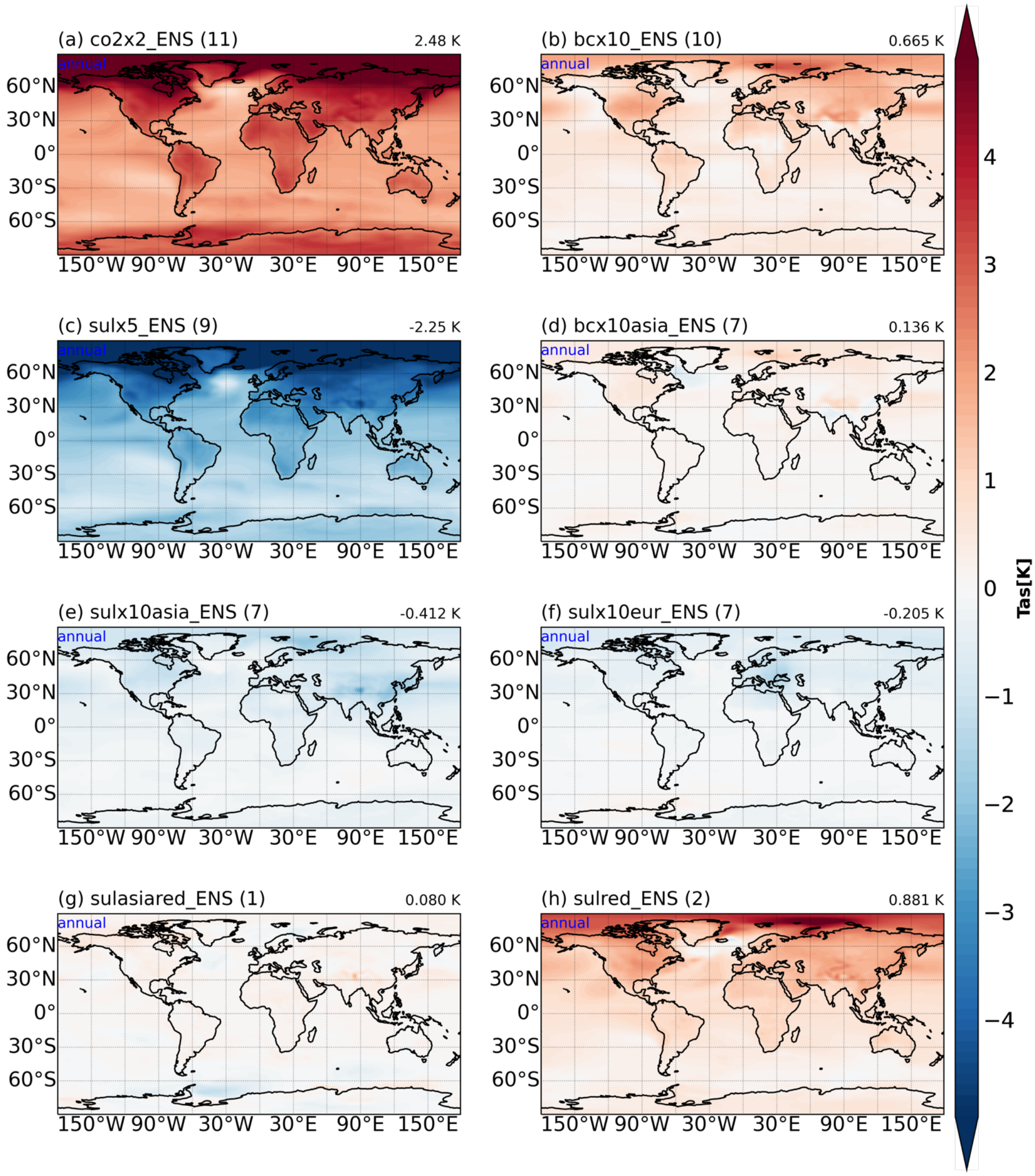

Figure 2: Spatial distribution of ensemble mean of annual near surface temperature responses (K) in (a) $co_2\times2$, (b) *bc×10*, (c) *sul×5*, (d) *bc×10asia*, (e) *sul×10asia*, (f) *sul×10eur*, (g) *sulasiared* and (h) *sulred* with respect to their base experiments. The values in the brackets represent number of models carried out the experiment. The ensemble means of change in annual near surface temperature for each perturbed experiment is given on the top right corner.

https://doi.org/10.5194/egusphere-2023-1605
Preprint. Discussion started: 15 August 2023

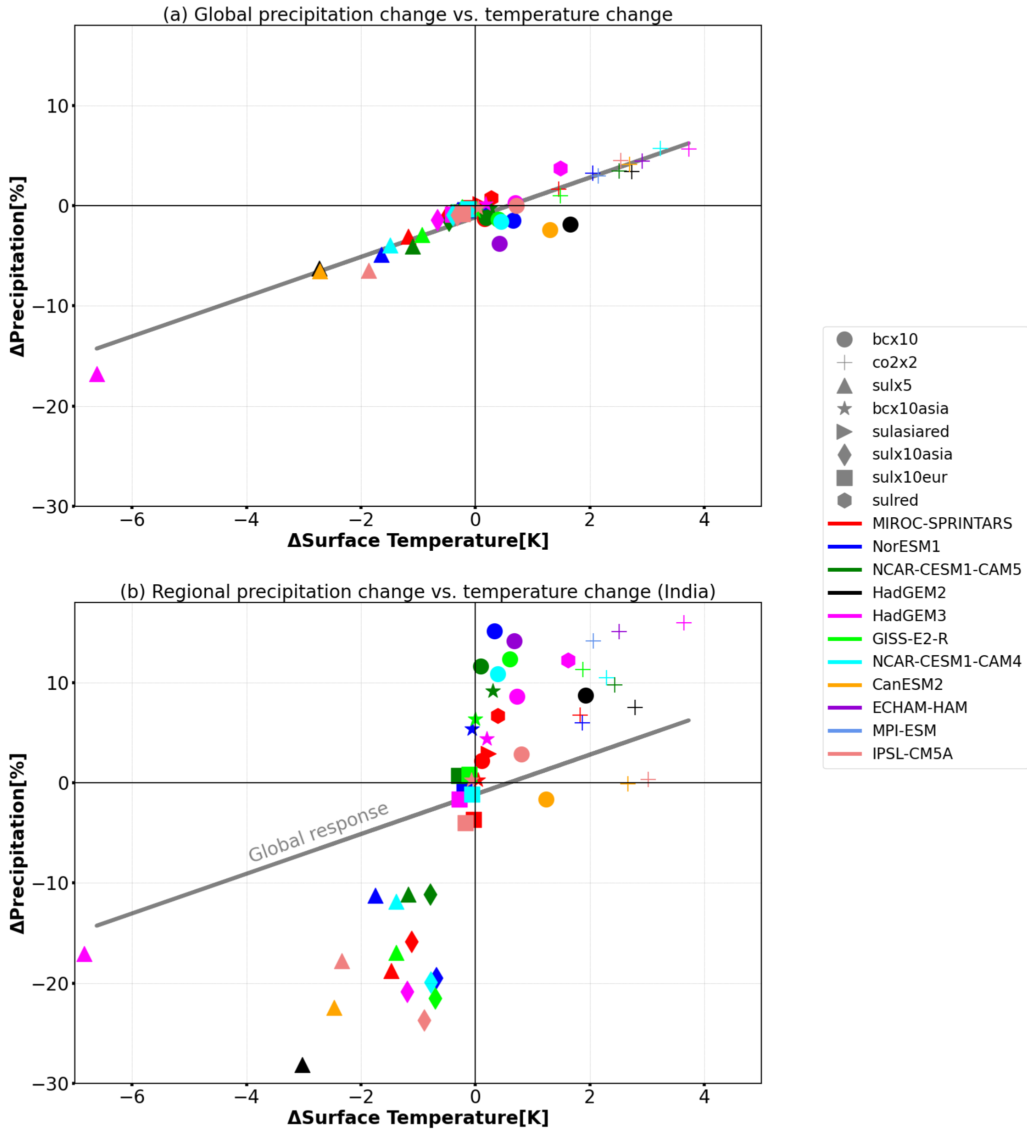

Figure 3: Scatter plot of the percentage change in the (a) global mean precipitation (%) vs. the change in the global near surface temperature (K) and changes in (b) regional precipitation (%) vs. changes in the near surface temperature (K) over India for all the perturbed model experiments.

https://doi.org/10.5194/egusphere-2023-1605
Preprint. Discussion started: 15 August 2023

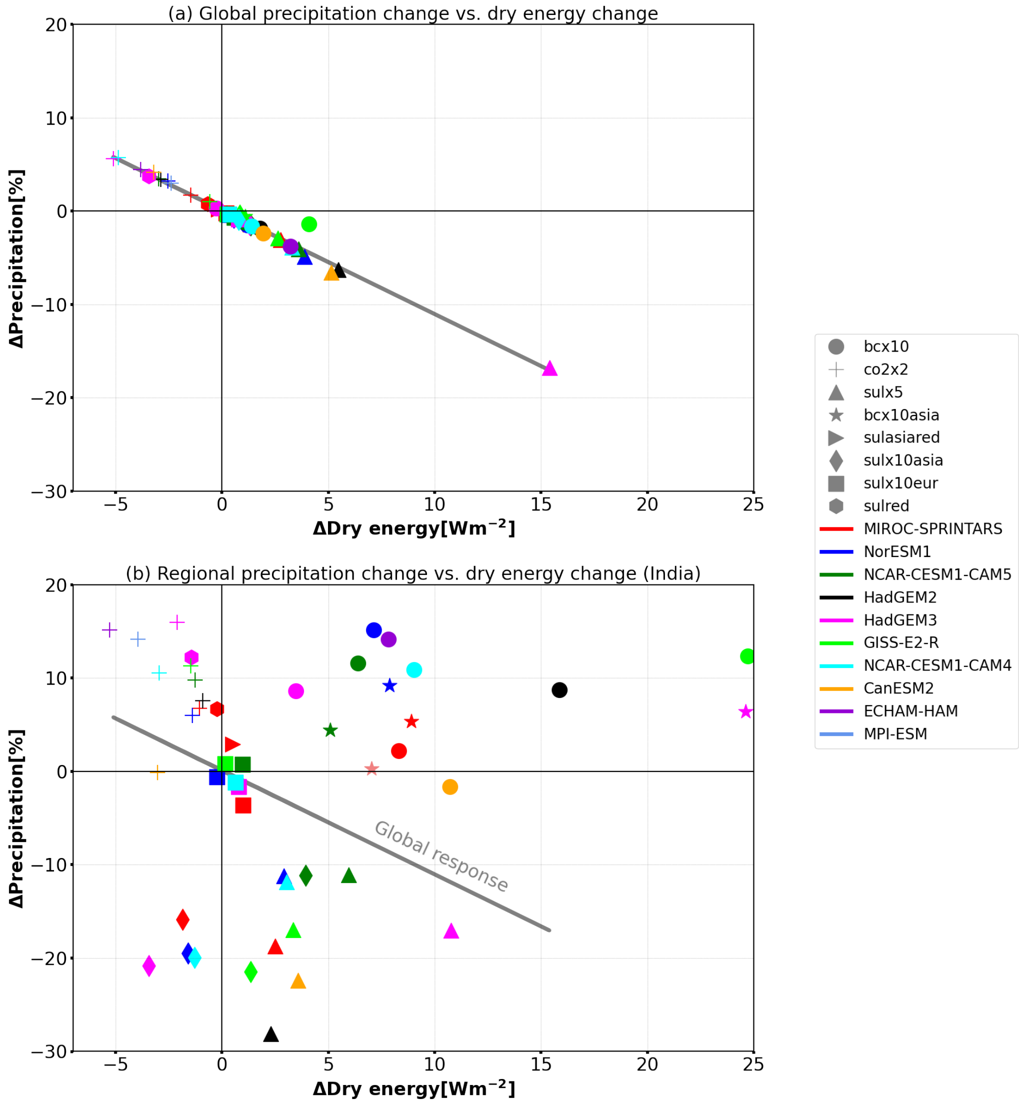

Figure 4: Scatter plot of the percentage change in the (a) global mean precipitation (%) vs. the global changes in the dry energy (Wm^{-2}) and changes in the (b) regional precipitation (%) vs. regional changes in the dry energy (Wm^{-2}) over India for all the perturbed model experiments.

https://doi.org/10.5194/egusphere-2023-1605
Preprint. Discussion started: 15 August 2023

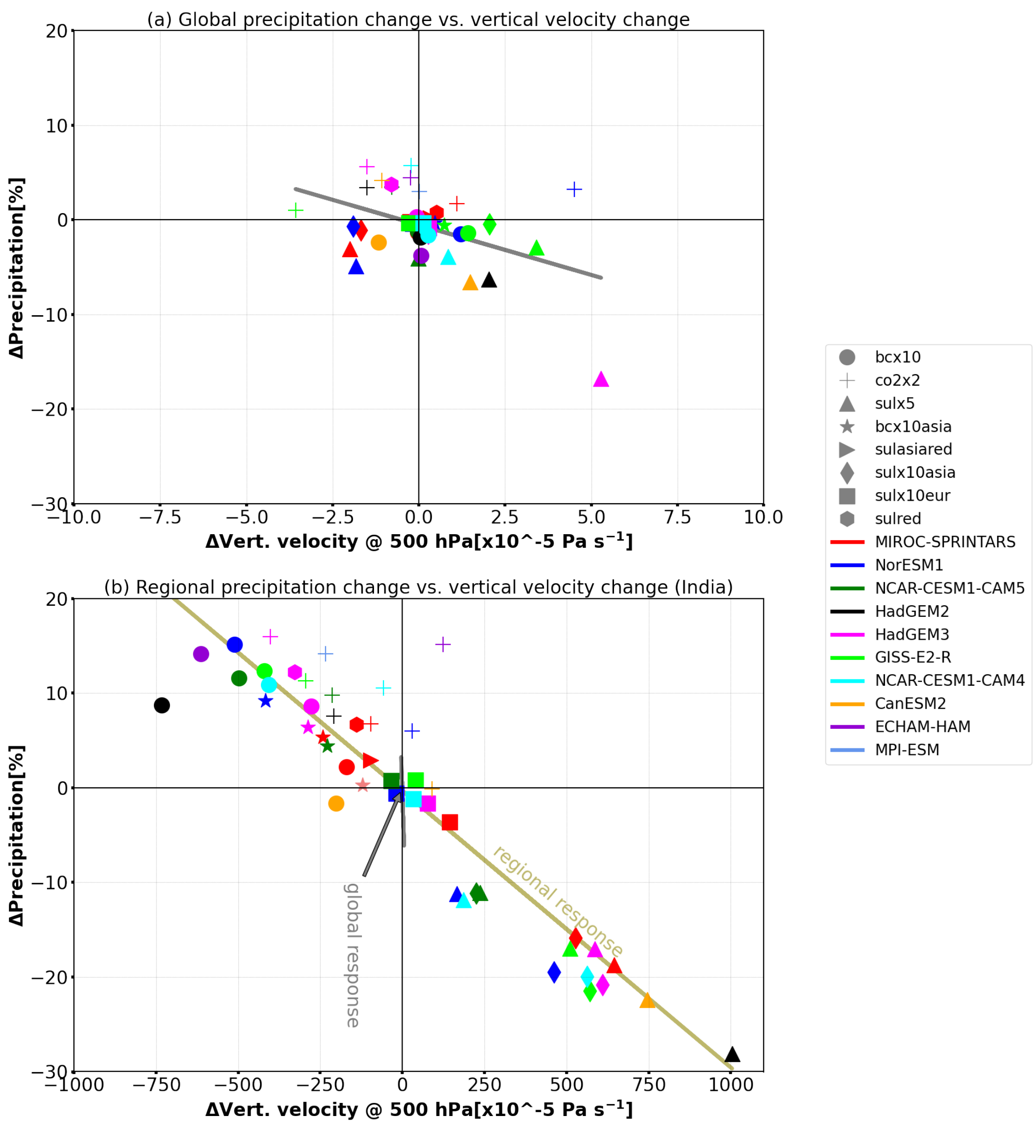

Figure 5: Scatter plot of the percentage change in the (a) global mean precipitation (%) vs. the changes in the global mean vertical velocity at 500 hPa (Pa s^{-1}) and changes in the (b) regional precipitation (%) vs. changes in the regional mean vertical velocity over India at 500 hPa (Pa s^{-1}) for all the perturbed model experiments.

https://doi.org/10.5194/egusphere-2023-1605
Preprint. Discussion started: 15 August 2023

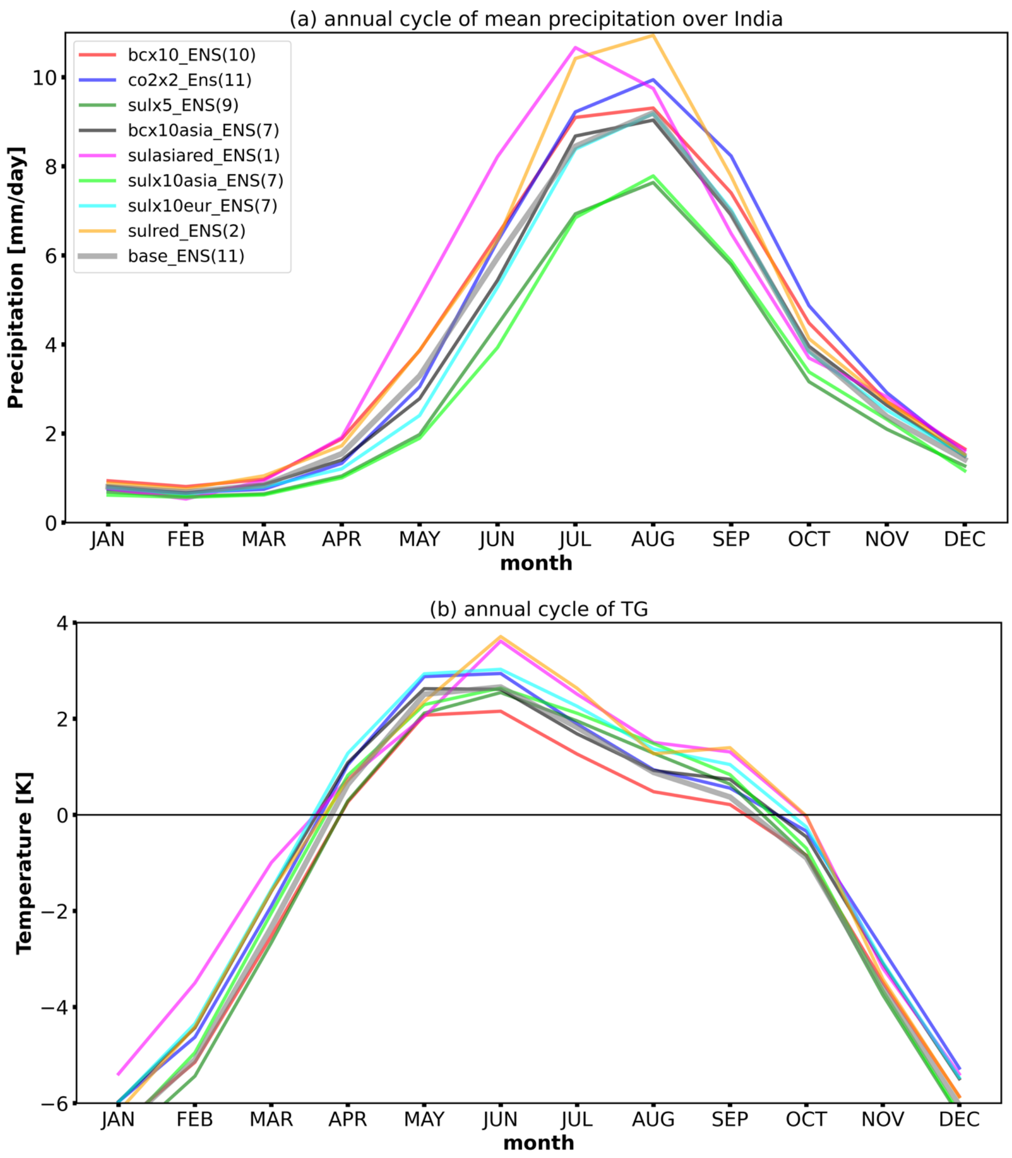

Figure 6: Annual cycle of (a) ensemble mean precipitation over India for all the model experiments. (b) Annual cycle of temperature gradient calculated by by taking difference between the surface temperature over Indian land mass (70–85°E, 10–30°N) and western Indian Ocean (50–65°E, 5°S-10°N) for all the model experiments. The number in the brackets depicts number of models carried out the particular perturbed experiment.

https://doi.org/10.5194/egusphere-2023-1605
Preprint. Discussion started: 15 August 2023

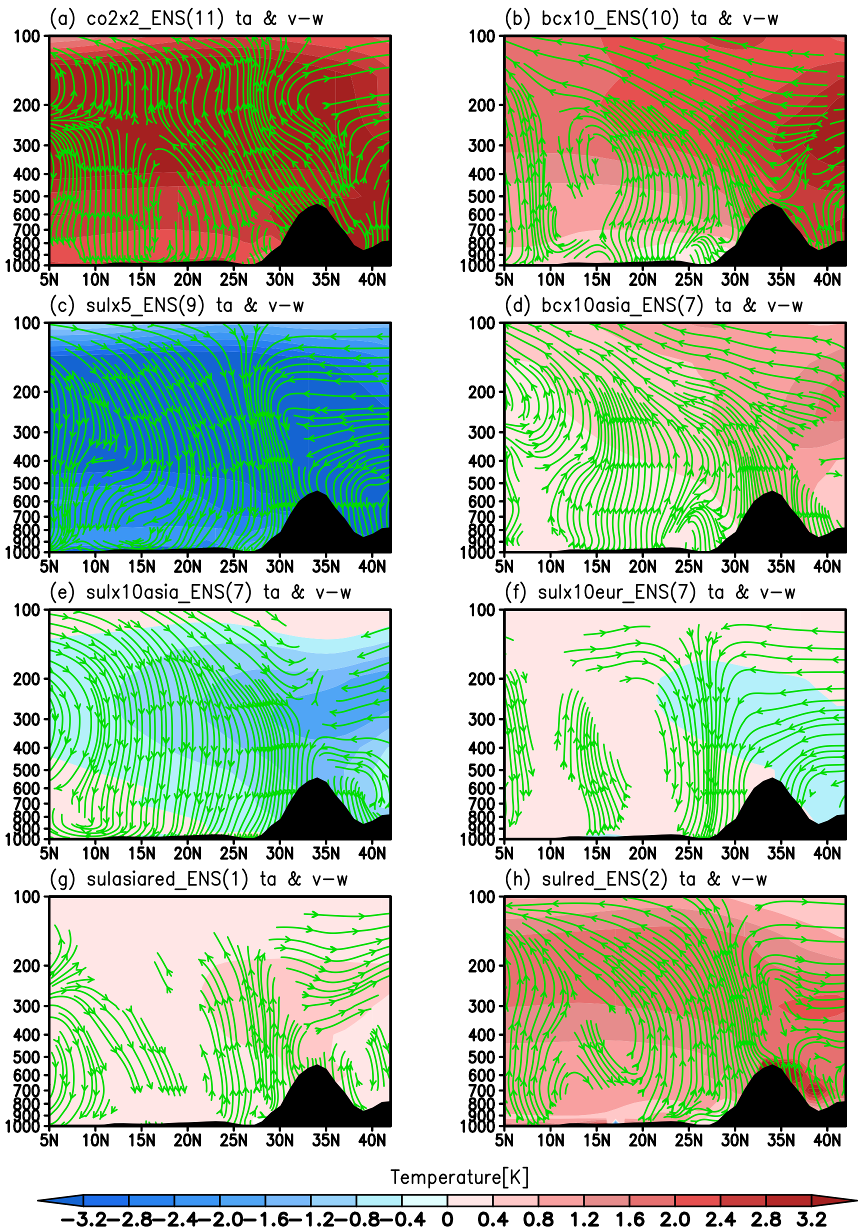

Figure 7: Vertical cross-section averaged over longitudes (68°E–98°E) showing total responses in ensemble mean of air temperature (shaded; units: - K) and meridional circulation (green contours) induced in (a) *co$_2$×2*, (b*) bc×10*, (c) *sul×5*, (d) *bc×10asia*, (e) *sul×10asia*, (f) *sul×10eur*, (g) *sulasiared* and (h) *sulred* with respect to their base experiments during the

https://doi.org/10.5194/egusphere-2023-1605
Preprint. Discussion started: 15 August 2023

Indian summer monsoon period. The number in the brackets depicts number of models carried out the particular perturbed experiment.

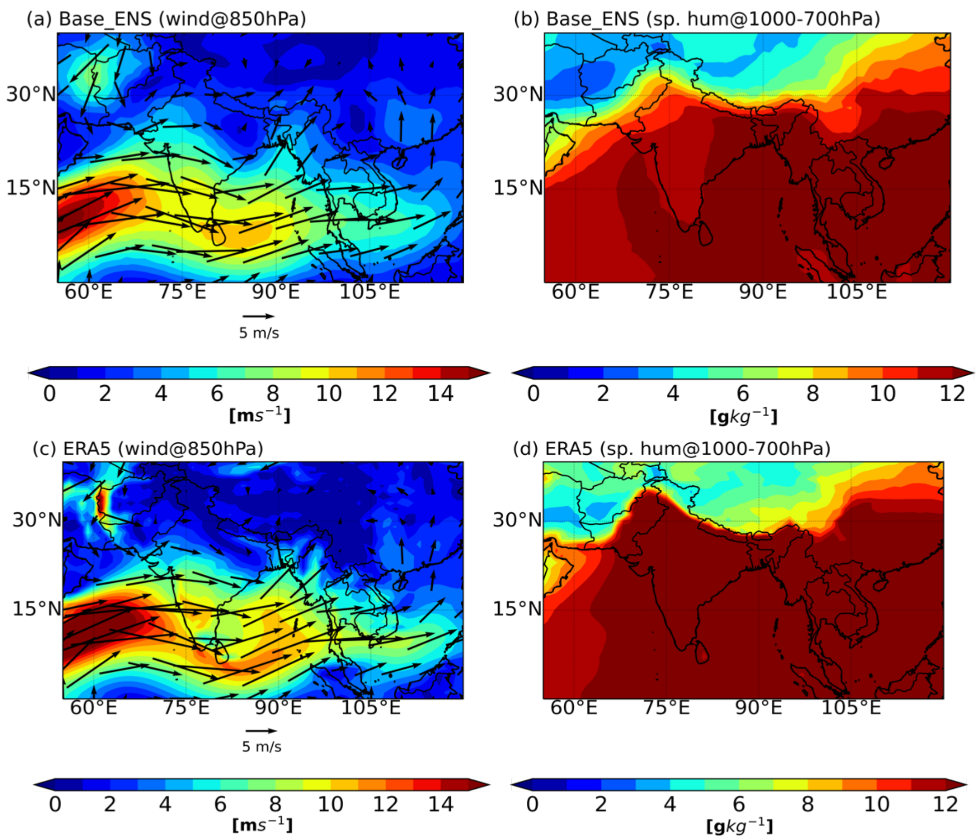

Figure 8: Spatial distribution of ensemble mean of (a, c) wind circulation at 850 hPa and (b, d) vertically averaged specific humidity (1000-700 hPa) considering all model base experiments (top panel) and ERA5 (bottom panel) respectively during the Indian summer monsoon season.

https://doi.org/10.5194/egusphere-2023-1605
Preprint. Discussion started: 15 August 2023

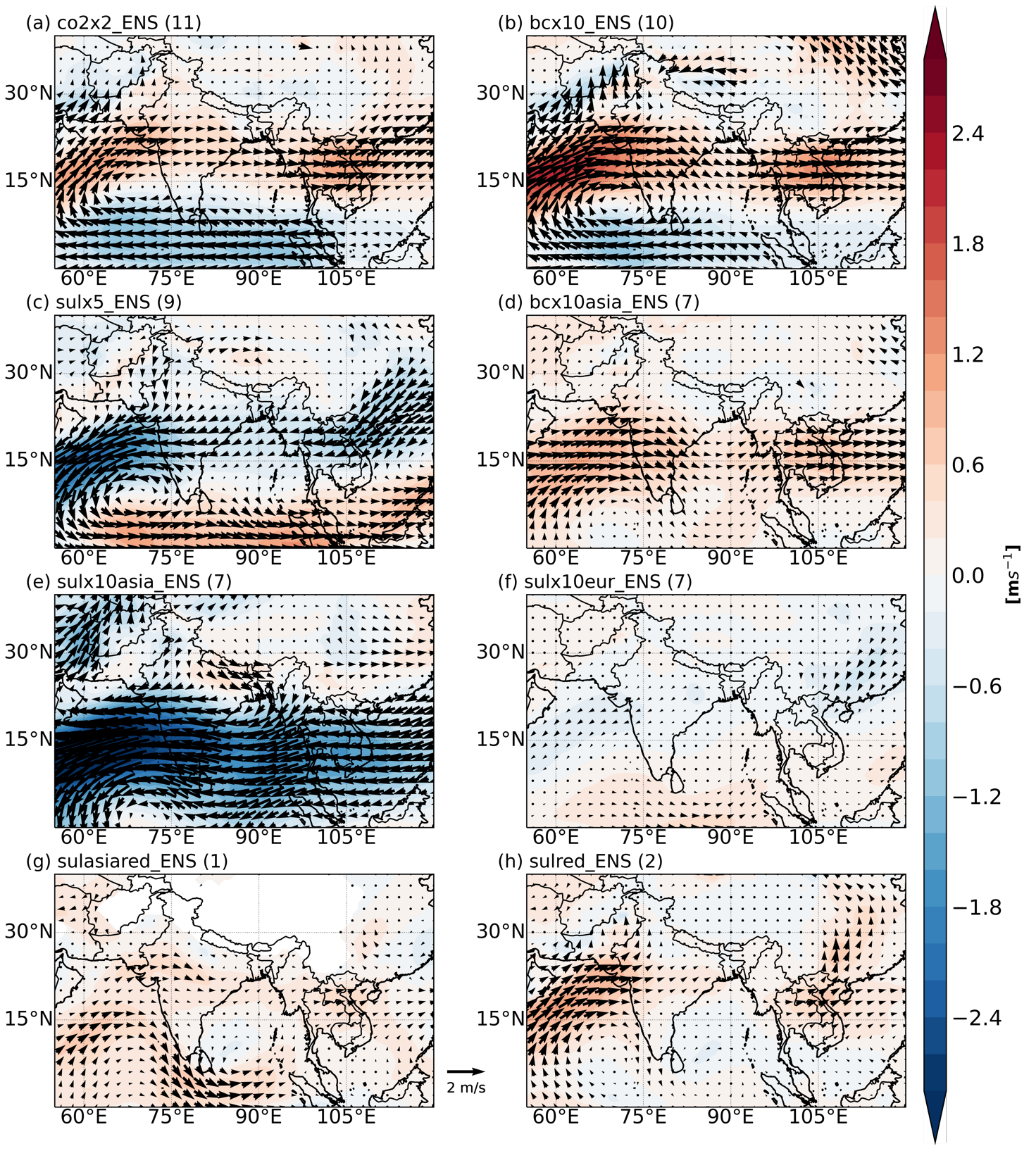

Figure 9: Spatial distribution of total responses in the ensemble mean of wind circulation (m/s) at 850 hPa in (a) *co$_2$×2*, (b) *bc×10*, (c) *sul×5*, (d) *bc×10asia*, (e) *sul×10asia*, (f) *sul×10eur*, (g) *sulasiared* and (h) *sulred* with respect to their base experiments during the Indian summer monsoon season. The number in the brackets depicts number of models carried out the particular perturbed experiment.